Supplementary Data

Table S1 Division of fluorescence spectral regions (Ritigala et al., 2021)

Region	Organic species
I	Tyrosine-like
II	Tryptophan-like
III	Fulvic-like
IV	Soluble microbial byproducts
V	Humic-like

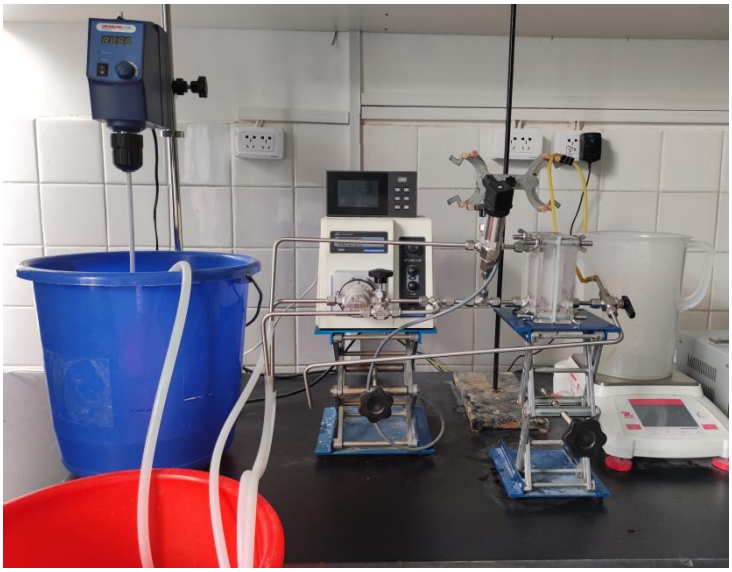

Fig. S1 Digital photo of the experimental device

Figure S1 shows the experimental device, including coagulation unit (electronic counting agitator, coagulation tank) and filtration unit (feeding tank, filtrate tank, membrane module, pump, electronic balance and counting computer). This system was constructed for surface water/coagulated effluent treatment by ceramic/polymeric membrane. PTC or PAC was used as the coagulant for coagulation before filtration. Detailed descriptions of the system operation are provided in Section 2.3.

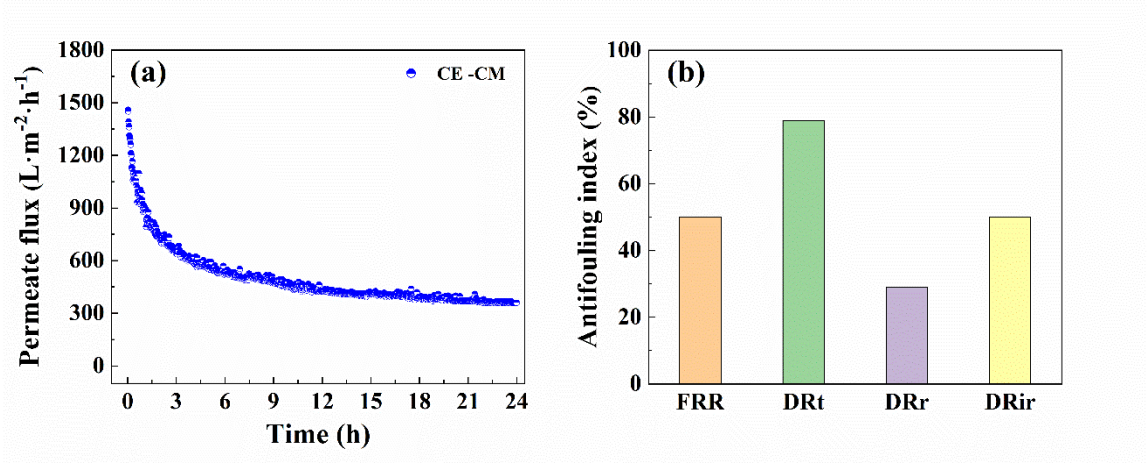

Fig. S2 (a) Permeate flux variation of ceramic membrane during 24 h filtration of PTC coagulation effluent under the dosage of 50 mg Ti/L and (b) antifouling indexs of ceramic membrane

Figure S2 displays permeate flux variation and antifouling index of ceramic membrane. In this experiment, PTC coagulated effluent was utilized as feed water to test the long-term operation stability and antifouling performance of ceramic membrane. Before filtrating the PTC coagulated effluent, deionized (DI) water was filtrated for 1 h under 30 kPa using ceramic membrane to obtain pure water flux J_{w1}. In the following, the stable flux of PTC coagulated effluent was measured at 30 kPa and recorded as J_p. Finally, the pure water flux of the ceramic membrane cleaned by scrubbing and ultrasonic cleaning was tested again at 30 kPa, and recorded as J_{w2}. The antifouling indexs including flux recovery ratio (FRR), total flux decline (DRt), reversible flux decline ratio (DRr) and irreversible flux decline ratio (DRir) were applied to judge the antifouling performance of ceramic membrane and calculated as follows.

$$FRR = \frac{J_{w2}}{J_{w1}} \times 100\% \quad , \qquad (S1)$$

$$DRt = \frac{J_{w1} - J_p}{J_{w1}} \times 100\% \quad , \qquad (S2)$$

$$DRr = \frac{J_{w2} - J_p}{J_{W1}} \times 100\% \quad , \qquad (S3)$$

$$DRir = \frac{J_{w1} - J_{w2}}{J_{w1}} \times 100\% \quad , \qquad (S4)$$

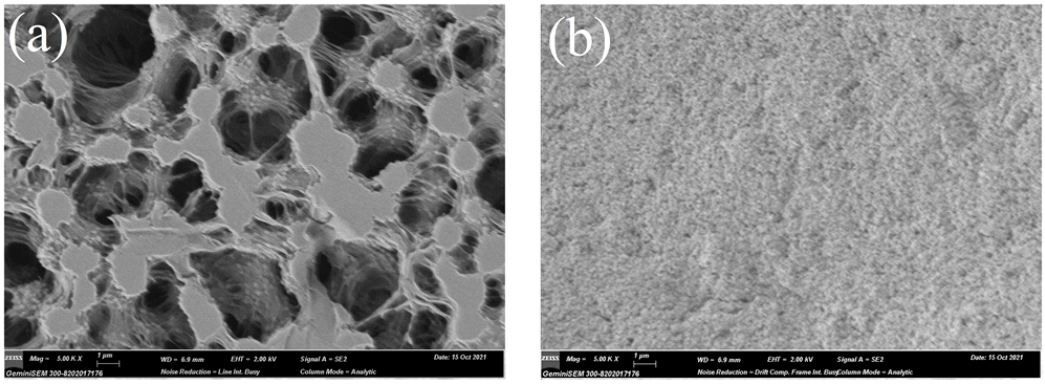

Fig. S3 SEM images of organic membrane surface: (a) virgin membrane; (b) fouled membrane after filtrating PTC coagulated effluent under the dosage of 50 mg Ti/L

As shown in Fig. S3, the surface of the original clean organic membrane was been covered by a cake layer evolved from flocs and contaminants after 10 hours of filtration. Compared with the ceramic membrane after filtrating PTC coagulated effluent shown in Fig. S4, the organic membrane formed a denser cake layer.

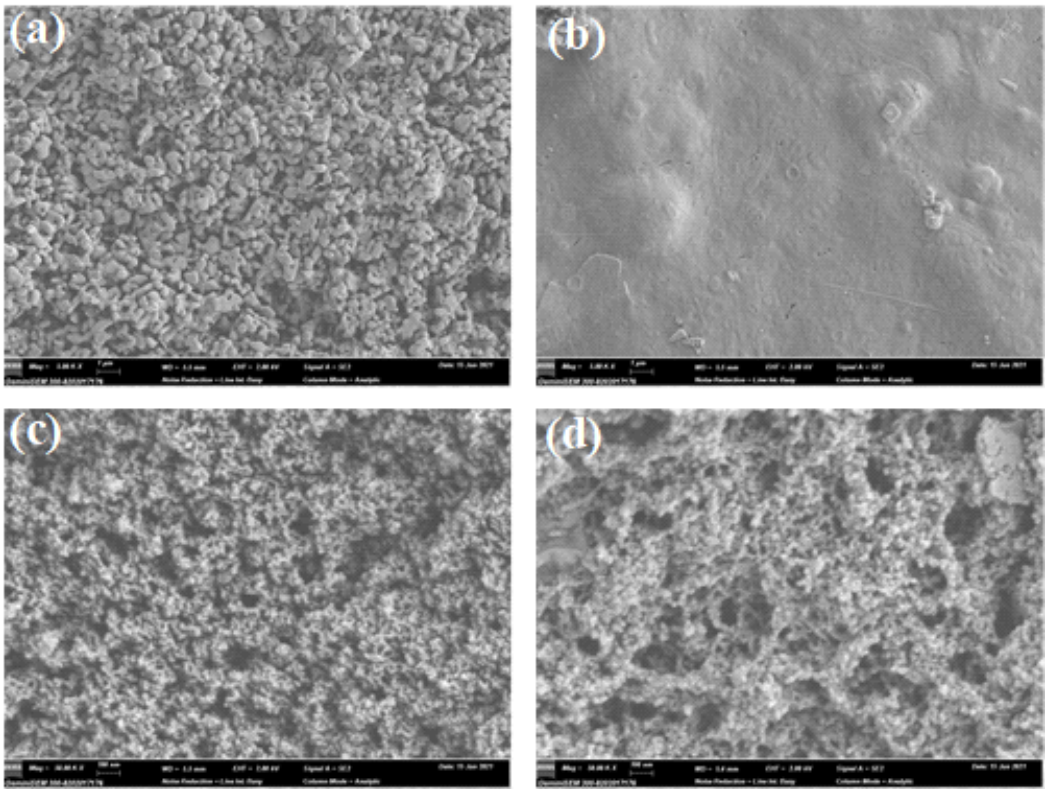

Fig. S4 SEM images of ceramic membrane surface: (a) virgin membrane, fouled membrane after filtrating (b) raw water, (c) PTC coagulated effluent and (d) PAC coagulated effluent (dosage of 50 mg Ti/L and 40 mg Al/L were selected for PTC and PAC coagulation, respectively)

As can be seen from Fig. S4, the most serious membrane pollution that the membrane hole has been completely blocked occurred on the membrane fouled by raw water, while the membrane fouling formed by PTC/PAC coagulated effluent was slighter than that of raw water. Although the surface of the membranes was deposited by flocs, there were many permeation channels in the membrane fouled by coagulation effluent. Compared with PAC, the flocs produced by PTC coagulation distributed more homogeneously on the surface of the membrane, while the flocs showed agglomeration in the case of PAC.

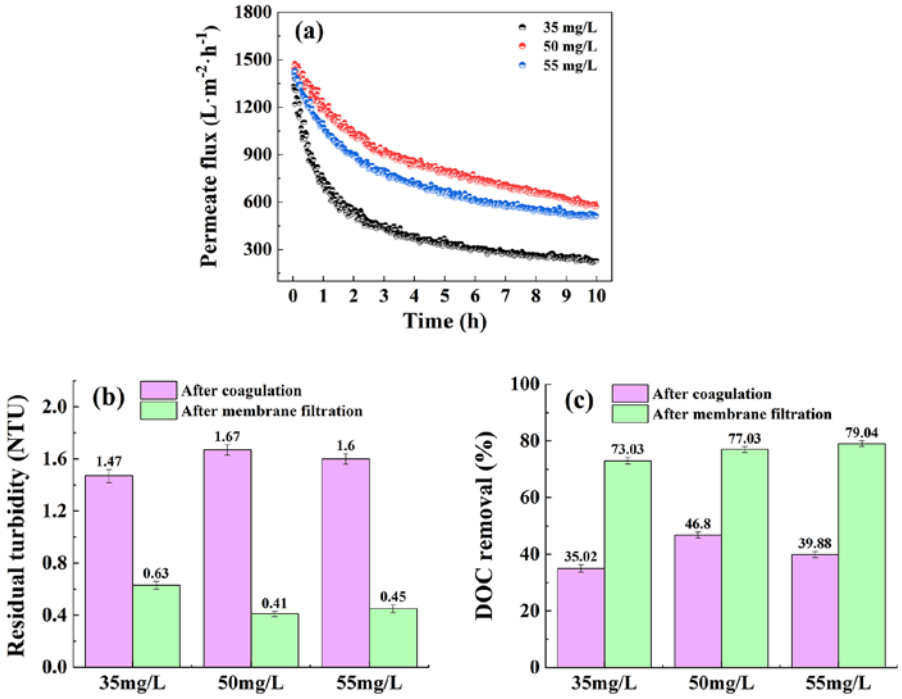

Fig. S5 Permeate flux and effluent quality before and after filtration with ceramic membrane under PTC varied dosage conditions: (a) permeate flux; (b) residual turbidity; (c) removal of dissolved organic matter

Figure S5 exhibits the permeate flux and the removal of organic pollutants and turbidity before and after filtration with ceramic membrane under varied dosage conditions of polytitanium chloride (PTC). Coagulant dosage significantly affected both permeate flux and effluent quality. Optimization of PTC dosage for practical practice was absolute necessary in terms of both permeate flux and organic removal. The permeate flux in equilibrium phase followed the order of 50 mg/L>55 mg/L>35 mg/L. The removal rate of DOC after filtration reached 77.0% at 50 mg/L. Compared with coagulation only, post-filtration resulted in the increase of DOC removal by 38.01%, 30.23% and 39.16% at 35 mg/L, 50 mg/L and 55 mg/L, respectively. According to J/J_0 in Fig. S6, the ceramic membrane was polluted most seriously at 35 mg/L, which could be

attributed to the higher residual turbidity and more residual dissolved organic matter in the coagulated effluent than the cases of 50 mg/L and 55 mg/L (Fig. 1).

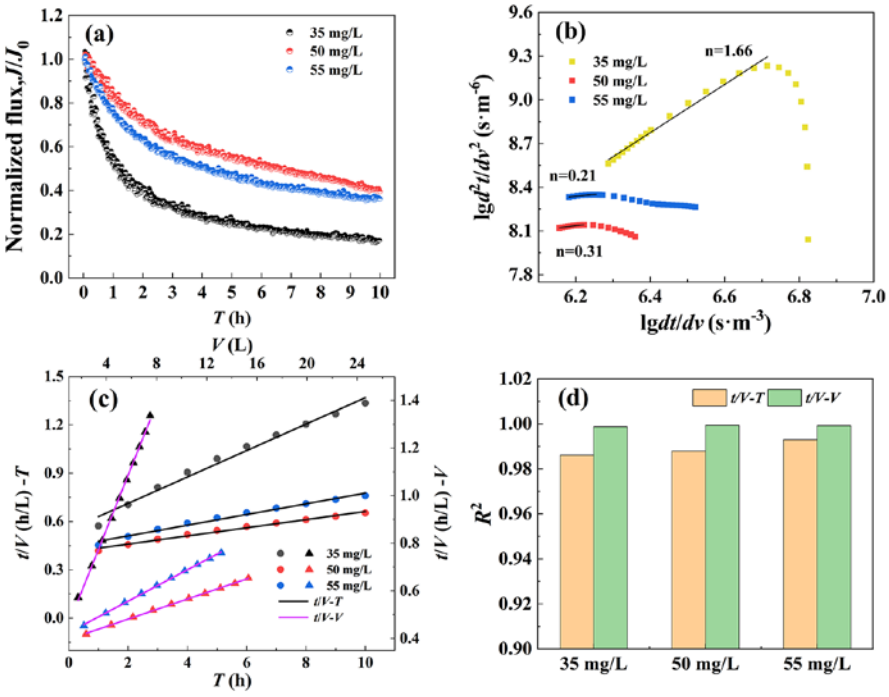

Fig. S6 Comparative analysis of membrane fouling mechanism according to mode 1, 2 and 3 under varied PTC dosages: (a) model 1: normalized flux (J/J_0) vs. filtration period; (b) model 2: fitting curves of lgd^2t/dV^2 vs. lgdt/dV; (c) model 3: fitting curves of t/V vs. T and t/V vs. V; (d) correlation parameters (R^2) of fitting curves for model 3

Figure S6 presents the fitting curves of membrane fouling according to three membrane fouling models at different PTC dosages. The dominant mechanism of membrane fouling was not the same under different dosages. It was concluded from model 3 and model 4 that the membrane fouling behavior under the three PTC dosages were all dominated by filter cake layer blocking when the entire time period was selected as the research object. By means of model 2, it can be seen that membrane fouling at 35 mg/L was dominated by standard blocking, i.e., membrane pore absorption, while that of 50 mg/L and 55 mg/L was dominated by cake filtration in the initial filtration period. The n values of 50 mg/L and 55 mg/L were 0.21 and 0.31, respectively. It can be speculated that cake blocking in case of 55 mg/L was more serious than that in the case of 50 mg/L. This was also confirmed by the fact that J/J_0 value at 55 mg/L was smaller than that at 50 mg/L in Fig. S6(a). The more serious cake layer pollution means that the ability to removal dissolved organic matter is stronger. Furthermore, it also explained why the permeate flux of 55 mg/L was smaller than 50 mg/L in Fig. S5(a). On the whole, the permeate flux increased with the reduction of membrane fouling, indicating membrane fouling mechanism has a significant effect on the permeation flux.

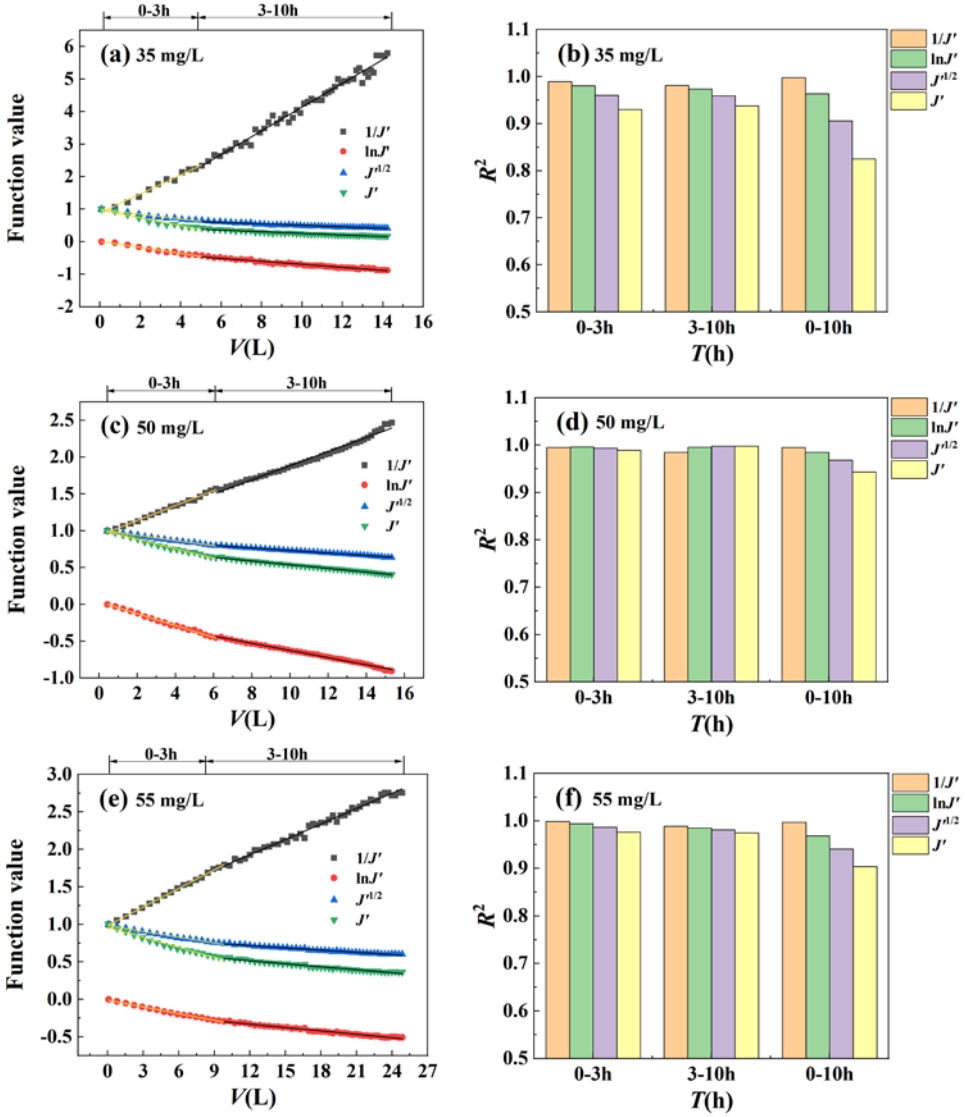

Fig. S7 Fitting curves (a, c, e) and correlation parameters (R^2) (b, d, f) of model 4 under three PTC dosage conditions: (a,b) 35 mg/L; (c,d) 50 mg/L; (e,f) 55 mg/L

Figure S7 displays characteristic curves of membrane fouling mechanism in different time periods. The analysis results confirm that the laws of membrane fouling mechanism under three dosages were consistent. In the time quantum of 0–3 h and 3–10 h, membrane fouling was the combination of several membrane fouling mechanisms. The membrane fouling behavior under the three PTC dosages were all dominated by filter cake layer blocking when the entire time period was selected as the research object.

References

Ritigala T, Demissie H, Chen Y, Zheng J, Zheng L, Zhu J, Fan H, Li J, Wang D, Weragoda S K, Weerasooriya R, Wei Y (2021). Optimized pre-treatment of high strength food waste digestate by high content aluminum-nanocluster based magnetic coagulation. Journal of Environmental Sciences-China, 104: 430–443